External and internal EGFR-activating signals drive mammary epithelial cells proliferation and viability

External and internal EGFR-activating signals drive mammary epithelial cells proliferation and viability

Alessia Morato [a], Eugenio Martignani [a], Silvia Miretti [a], Mario Baratta [a] and Paolo Accornero [a *]

1 Department of Veterinary Science, University of Turin, Grugliasco (TO), Italy

Corresponding author: * Paolo Accornero, Department of Veterinary Science, University of Turin, Largo Braccini 2, 10095, Grugliasco (TO), Italy; Tel. +39 011 6709326; Fax. +39 011 6709138; email: paolo.accornero@unito.it

Highlights

- EGFR autocrine signaling drive mammary epithelial cell proliferation and cell cycle
- An EGFR-dependent Erk 1/2 phosphorylation is active in cells cultured in growth factor deprived medium
- Krt14 negative / Krt18 positive mammary cells depend on EGFR activation for survival
- Mammary cells express high mRNA levels of two or more EGFR ligands

Abtract

During puberty, the mammary gland undergoes an intense growth, dependent on the interplay between the Epidermal Growth Factor Receptor (EGFR) in the stroma and different mammary epithelial receptors. We hypothesize that EGFR expressed in the mammary epithelium also has a role in puberty and the epithelial cells can self-sustain by EGFR-mediated autocrine signaling. We adopted mammary cell lines from different species, as *in vitro* model for the epithelium, and we observed that EGFR-signaling positively affects their survival and proliferation. Once deprived of external growth factors, mammary cells still showed strong Erk 1/2 phosphorylation, abolished upon EGFR inhibition, coupled with a further reduction in survival and proliferation. Based on gene expression analysis, three EGFR-ligands (AREG, EREG and HBEGF) are likely to mediate this autocrine signaling. In conclusion, internal EGFR-activating signals sustain mammary epithelial cell proliferation and survival *in vitro*.

Keywords: Mammary gland; EGFR; EGFR-ligands; autocrine; Erk 1/2; keratin 14/18

Abbreviations: Epidermal Growth Factor Receptor = EGFR; amphiregulin = AREG; epiregulin = EREG; heparin-binding EGF-like growth factor = HBEGF; Keratin 14 = Krt14; Keratin 18 = Krt18.

Acknowledgments: We are grateful to Cristina Cecere for technical assistance.

Funding: This work was supported by national grants from Ministry of Instruction, University and Research and by local grants from Università di Torino. The funders had no role in study design, data collection and analysis, decision to publish, or preparation of the manuscript.

1. Introduction

The mammary gland develops through a complex sequence of events, which start in the embryonic period and culminate towards the end of pregnancy. In the prepubertal period, the mammary morphogenesis is based on a close interaction between the epithelial and the stromal compartments, and the ductal tree grows isometrically with the rest of the body. After puberty, endocrine stimuli are the main drivers of mammary development and the ductal tree undergoes a robust allometric growth. In the murine species, specific club-shaped structures, known as Terminal End Buds (TEBs), make way to the progression of the ductal tree into the surrounding fat pad. Ovarian estrogens trigger this impressive elongation via Estrogen Receptor α (ERα) expressed in a subset of epithelial cells: ERα-positive cells release amphiregulin (AREG), via TACE-shedding (tumor necrosis factor-α-converting enzyme also known as ADAM17), which binds EGFR in the stromal compartment. Activated stromal cells release other growth factors (mainly FGFs) which in turn stimulate both ER-positive and ER-negative epithelial cells (Ciarloni et al., 2007; Macias & Hinck, 2012; Zhang et al., 2014). Since only the stromal fraction of EGFR was proved essential for the ductal elongation, ERα-negative cells are thought to proliferate through the interplay with the stroma (Sternlicht et al., 2005; Wiesen et al., 1999).

The ErbB tyrosine kinase receptor (RTK) family comprises four members: Erb-B1 (EGFR), Erb-B2, Erb-B3 and Erb-B4. During the pubertal development of the murine mammary gland, EGFR is highly expressed in the stroma, and to a lesser extent in the epithelial TEBs and ducts. Erb-B2 is mostly present in the epithelium, but being an orphan receptor, requires a heterodimerization shedding for its activation. Erb-B3 is only detectable when the mammary gland is mature, while Erb-B4 can be detected during pregnancy and lactation (Schroeder & Lee, 1998; Spivak-Kroizman et al., 1992). EGFR can be activated upon the binding of seven different peptides of the EGF-family: amphiregulin (AREG), betacellulin (BTC), epidermal growth factor (EGF), epigen (EPGN), epiregulin (EREG), heparin-binding EGF-like growth factor (HBEGF) and transforming growth factor α (TGFα) (Harris et al., 2003). Overall AREG is more expressed during puberty than in the following stages of development (D'Cruz et al., 2002; Schroeder & Lee, 1998) and displays a significantly higher expression in the TEBs and in the ducts compared to the stroma, in contrast to other EGFR-ligands that are variably expressed in the mammary epithelium (DiAugustine et al., 1997; Sternlicht et al., 2005).

Elegant studies performed on knock-out mice have shed light on many mechanisms of the pubertal mammary morphogenesis, concluding that epithelial EGFR and EGF-related peptides different from AREG have a dispensable role during this period of growth (Ciarloni et al., 2007; Luetteke et al., 1999; Sternlicht et al., 2005). Good evidence exists that the interaction between epithelial EGFR and EGF-like ligands has also a direct (i.e not mediated by stroma) effect on the epithelial cells themselves: immature mammary epithelial organoids undergo a prominent branching in the presence of EGF, TGFα, HBEGF and AREG (Camacho Leal et al., 2012; Jenkins et al., 2012; Simian et al., 2001; Sisto et al., 2017). Although EGFR is primarily a stromal receptor, it is also present in the epithelial compartment, especially in the cap cells of the end buds and in the myoepithelial cells of the mammary ducts (Coleman et al., 1988; DiAugustine et al., 1997). All that considered, it could be speculated that the expression of AREG (or other EGF-like growth factors) is also induced locally (independently from any systemic hormones). It is also possible that these growth factors act locally, activating EGFR expressed by the epithelium itself. In other words, an autocrine activity within the mammary epithelium can be hypothesized (graphical abstract, right panel), whereby mammary epithelial cells can sustain their own proliferation by releasing EGF-like growth factors that activate EGFR expressed locally. An autocrine signaling, though dispensable for the growth of the mammary tree, might contribute to its normal development, together with the previously mechanism (graphical abstract, left panel), based on a stromal-epithelial interplay, that other authors previously described (Ciarloni et al., 2007; Sternlicht et al., 2005).

Another open question is whether the information achieved in the murine species can be translated to other animal models. Although not much is known about the distribution of ErbB and growth factors in the mammary gland of other species, their pattern of expression could substantially diverge from what described for the mouse. For instance, in the pubertal rat the TEBs, more than other structures, express EGFR, as well as Erb-B4 which is commonly considered a receptor of the pregnant mammary gland, in the mouse (Darcy et al., 1999, 2000). One might therefore speculate that also the relative importance of ErbB and growth factors in the normal development of the pubertal mammary gland could differ, in other species. Still, most of the studies on the morphogenesis of the mammary gland have been performed on murine models. This represents a substantial limit when data about the endocrine regulation of mammary development are needed in other species.

In the present study we sought to test our hypothesis. We chose to work *in vitro* with 4 different cell lines (human, murine, bovine), as a model for the mammary epithelium, for multiple reasons. First, to perform our experiments on a homogeneous population of epithelial cells, without any stromal interference. Second, to offer evidence valid in different species. Here we investigated the ability of our lines to sustain their own proliferation and to remain viable, even in the absence of external stimuli, in an EGFR-dependent way (autocrine activity). Since the Erk 1/2 pathway is known to have a pivotal function in cell viability and proliferation (Kerpedjieva et al., 2012; Thiel & Cibelli, 2002), downstream of EGFR (Camacho Leal et al., 2012; Fata et al., 2007; Kariagina et al., 2010), we subsequently verified whether the activation state of this pathway is involved in the autocrine activity of our cell lines, also investigating other pathways potentially activated in this scenario. To identify potentials mediators of the hypothesized autocrine model, we finally looked which EGFR ligands are transcribed by the cells and whether EGFR-dependent signaling regulate this expression.

2. Materials and Methods

2.1. Materials. All materials, unless otherwise stated, were from Merck KGaA (Darmstadt, Germany). DMEM, DMEM/F12, FBS and Hoechst 33342 were from Thermo Fisher Scientific (Waltham, MA, USA). Epidermal Growth Factor (EGF) was from Immunotools (Friesoythe, Germany). AG1478 and UO126 were from LC Laboratories (Woburn, MA, USA). Rabbit anti-Erk 1 (1:1000; sc-94), anti-EGFR (for murine cell lines 1:1000; sc-03-G) and anti-STAT5 (1:1000; sc-835) antibodies were from Santa Cruz Biotechnology (Santa Cruz, CA, USA); mouse anti-phospho-Erk 1/2 (1:5000; M 8159), mouse anti-Keratin 18 (Krt18; 1:200; K5-B) and mouse anti-α-tubulin (1:10000; T5168) antibodies were from Merck KGaA; rabbit anti-Keratin 14 (Krt14; 1:500 for immunohistochemistry and 1:2000 for western-blot; Poly19053) antibody was from BioLegend (Dedham, MA, USA); mouse anti-Erb-B2 (1:1000; CB11, MA1-35720) and rabbit anti-AREG (1:7500; PA5-16621) were from ThermoFisher Scientific; rabbit anti-Her2/Erb-B2 antibody (1:1000; A0485) was from Dako (Glostrup, Denmark); rabbit anti-EGFR (for human and bovine cell lines; 1:1000; # 2232); rabbit anti-phospho-EGFR (tyr-1068; 1:1000; # 2234), anti-phospho-Akt (ser-473; 1:1000; # 9271),

anti-phospho-STAT3 (tyr-705; 1:1000; # 9131), anti-phospho-STAT5 (tyr-694; 1:1000; # 9351), anti-Akt (1:2000; # 9272) and anti-STAT3 (1:2000; # 9132) antibodies were from Cell Signaling Technologies (Danvers, MA,USA). Alexa-fluor-488 goat-anti-rabbit and Alexa-fluor-594 goat-anti-mouse secondary antibodies were from Invitrogen Corporation (Carlsbad, Ca, USA).

2.2. Cell culture. HC11 murine mammary epithelial cell line (ATCC n. CRL-3062) was cultured in DMEM with 10% FBS, 10 ng/mL EGF and 5µg/mL insulin**.** NMuMG murine mammary epithelial cell line (ATCC n. CRL-1636) was kindly provided by Dr. Montesano R. (University of Geneva Medical School, CH) and cultured on collagen coated plates in DMEM with 10% FBS. MCF-10A human mammary epithelial cell line (ATCC n. CRL-10317) was cultured in DMEM/F12 with 5% Horse Serum (HS), 20 ng/mL EGF, 10 µg/mL insulin, 0.5 µg/mL hydrocortisone, 100 ng/mL cholera toxin. The BME-UV bovine mammary epithelial cell line was kindly provided by Dr. Politis I. (Agricultural University of Athens, Athens, GR) and cultured in DMEM with 10% FBS, 10 ng/mL EGF and 1:100 ITS liquid media supplement.

2.3. 3D collagen assay. Collagen gels were obtained preparing a gel solution by mixing, in an ice bucket, 3,15 parts of H_2O, 1 part of DMEM 10x, 0,25 parts of Hepes (1 M, pH 7,4), 1 part of $NaHCO_3$ (22 g/liter), 1 part of Fetal Bovine Serum, 0,6 parts of NaOH (0,1N) and 3 parts of Rat type I collagen (final approximate concentration of 1,5 mg/mL). 250 µL of solution were let gel at the bottom of each well (24 well plate) at 37° C for 20 min. Cells were trypsinized, resuspended in complete medium and counted. Each well was filled with 0,5 ml collagen solution ($2,5 \times 10^3$ cells) and let gel at 37° C for 25 min. Then, 1 mL of complete medium was slowly added to each well. Cells were allowed to grow for 4 days, then the medium was delicately replaced with new medium containing the indicated inhibitors/factors. After 48 h gels were photographed with a Leica AF6000 LX inverted microscope.

2.4. Flow cytometry. Cells were seeded on 6 cm dishes at a density of 300.000 cells/well in their specific growth medium. Following 6 h of culture, the medium was replaced with the treatment medium as indicated and cells were let grow for different timepoints depending on the cell line and the experiment. Cells were washed 3 times with PBS and added with 500 µL of trypsin. Following cell detachment, 1,5 mL of DMEM with 10% FBS was added and cells were spinned at 250 x g for 5 min. Medium was carefully removed, 2 mL of PBS were added and cells were resuspended. Cells were then fixed by adding 2 mL of ethanol drop by drop and incubating 1 h at 4°C. Samples were then spinned at 500 x g for 7 min, resuspended in 1 mL of

PBS with 5 µg/mL DAPI and stained overnight at 4°C. The samples were analysed using an Attune Acoustic Focusing Cytometer (Invitrogen Corporation) equipped with a 405 nm (violet) excitation laser and a 405/40 nm (blue) emission filter. For each sample 25.000 to 50.000 events were analyzed and each experiment was repeated 3 or more times. The percentages of cells in the G0/G1 phase of their cycle were calculated using the Attune Cytometric Software version 2.1 (Invitrogen). For the gating procedure see Supplementary Fig. S1.

For the analysis of cell death, following culture, all the supernatant was collected and mixed with the trypsinized cells. The next steps were identical as above. At least 50.000 events were acquired and experiments were repeated 3 or more times. The percentage of Sub G0/1 was calculated by dividing the number of Sub G0/G1 events by number of FSC/SSC gated events. For the gating procedure see Supplementary Fig. S2.

2.5. Nuclei counting and MTT assay. Cells were seeded in 6 well-plates at a density of 300.000 cells/well, in growth medium (G). After 6 h, G was changed with the medium for each experimental condition. After 48 h (24 h for BME cells), the medium was removed and replaced with fresh culture medium, in preparation to the following experiments.

For the nuclei counting, Hoechst stain was added at a concentration of 5 µg/mL and pictures were taken with Nikon Eclipse Ti2, equipped with a DS-Qi2 digital camera, controlled by NIS-Elements software version 5.21. The microscope was programmed to scan 20 fields per condition. Cell profiler software ver. 3.1.8 (https://cellprofiler.org/) was used to count the nuclei (IdentifyPrimaryObject Module) and the average of 20 fields was calculated. Each experiment was repeated 3 times.

For the MTT assay, 3-(4,5-dimethylthiazol-2-yl)-2,5-diphenyltetrazolium bromide (MTT) was added at a concentration of 500 µg/mL and the plates were incubated at 37° C for 2 h. The cells were finally lysed with a solution of SDS 10% and HCl 0.04 M, and the absorbance of the lysate was measured at 570 nm with a reference at 655 nm. Each experiment was repeated 3 times.

2.6. Gene expression analysis. For RNA extraction **c**ells of each line were seeded in 6 cm dishes in growth medium for 6 h, then cultured for 16 h (HC11, NMuMG, MCF-10A) or 4 h (BME-UV) under the indicated experimental conditions. Cells were then lysed in 1 mL Tryzol and DNA-free total RNA was isolated following the manufacturer's protocol. 500 ng of RNA were reverse transcribed with iScriptTM

cDNA Synthesis Kit (Bio-Rad Laboratories). Reverse transcribed samples were diluted 1:20 in RNAse free water. For quantitative rt-PCR cDNA (7.5 ng) was amplified with a CFX Connect real-time PCR system (Bio-Rad Laboratories, Hercules, Ca, USA), using SsoAdvanced Universal SYBR Green Supermix (Bio-Rad Laboratories) following the manufacturer's protocol. Primers were concentrated 250 nM. Primers sequences and efficiencies are indicated in Supplementary Table S1. The expression of each analysed gene was normalized to hypoxanthine phosphoribosyl-transferase 1 (HPRT-1) and glyceraldehyde-3-phosphate dehydrogenase (GADPH) mRNA expression, which are constant in the cell lines under our experimental conditions except in the MCF-10A experiments in which only GAPDH was used because HPRT was not stable. Each amplification curve was corrected for efficiency of the corresponding gene, calculated by standard dilution curves. CFX Manager Software 3.1 (Bio-Rad Laboratories) was used for both gene expression analysis and efficiency calculation/correction.

2.7. Protein expression analysis. For protein extraction, cells were seeded in 6 cm dishes ($1x10^6$ cells per dish), for 6 h in G, then cultured under the indicated experimental conditions for 16 h (4 h for BME-UV). Dishes were washed with ice-cold PBS and lysed for 10' on ice, in 300 µl of a lysis solution (20 mM Tris pH 7.5, 150 mM NaCl, 1 mM EDTA, 1 mM EGTA, 1% Triton X 100, 1 mM glycerolphosphate), Protease Inhibitor Cocktail (1:100), 1 mM sodium orthovanadate, 1mM phenylmethylsulfonyl fluoride. Samples were scraped (Orange Scientific), collected, and centrifuged at 4°C for 10' at 13.000 rpm. Supernatants were quantified with a DC Protein Assay (Biorad Laboratories). For Western-Blot, samples (20-100 µg of total protein) were resolved on SDS-PAGE gels and transferred to 0,45 µm hybridization nitrocellulose filters (Millipore, Burlington, MA, USA). Membranes were blocked at RT for 1 h in a 10% BSA Tris-buffered saline (TBS, 10 mM Tris and 150 mM NaCl, pH 7.4) then incubated for 16 h at 4°C with the indicated primary antibodies. Membranes were washed in TBS–Tween then incubated for 1 h at room temperature with 1:10.000 diluted HRP-conjugated secondary antibodies (Thermo Fisher Scientific). The membranes were in TBS–Tween and incubated for five min at room temperature with Clarity Western ECL Substrate (Biorad Laboratories). The proteins were visualized by briefly exposing the membrane to an autoradiographic CL-XPosure Film (Thermo Fisher Scientific). Western Blot results were then acquired with an Epson scanner.

2.8. Immunocytochemistry. MCF-10A cells seeded in 6-well plates (200.000 cells per well) in G for 6 h then cultured under different conditions for 48 h. Culture medium was then removed and cells were fixed for 40'' in acetone/methanol solution (1:1). Culture dishes were washed with Tris Buffered Saline (Tris 0,1 M, NaCl 8g, pH 7,6) then incubated for 1 h with goat serum 10% in Antibody Dilution Buffer (ADB; TBS with BSA 1%, Na-azide 0,1%). Cells were then incubated with diluted Krt14 (1:500) and Krt18 (1:200) antibodies for 1 h at RT. Dishes were washed with TBS and incubated with Alexa-fluor-488 goat-anti-rabbit and Alexa-fluor-594 goat-anti-mouse secondary antibodies (5 µg/mL); after 60 minutes cells were washed in TBS and DAPI (5 µg/mL) was added for 15 minutes. Dishes were washed twice with TBS and pictures were acquired with a Leica AF6000 LX (Leica Microsystems, Wetzlar, Germany) fluorescent microscope equipped with a Leica DFC350FX digital camera controlled by the LAS AF software (Leica Microsystems). For every culture condition 16 randomly selected fields were acquired and every experiment was repeated three times. ImageJ software was used to determine the Krt14Area, the area positive for Krt14, by using the ImageJ Image_Adjust_Color threshold... command with a Brightness value set at constant value followed by the Analyze_Histogram command. The whole area occupied by cells (TOTarea) was determined using the area occupied by the Krt18 stained cells (all MCF-10A cells are positive). For this purpose, we used the ImageJ Adjust_Brightness/Contrast… to highlight cell boundaries, then the Wand tool to select the area of the plate covered by the cells (with the Freehand selections when isolated cells or group of cells needed to be selected manually), then the Edit_Selection_Make Inverse to select the area covered by cells and finally the Analyze_Measure tool to quantify this area. The average percentage value was obtained by dividing Krt14Area by the TOTarea. For an outline of the procedure see Supplementary Fig. S3. An example of the images used to produce the composites of Fig. 5 is present in Supplementary Fig. S10.

2.9. Statistics. The analysis was performed with SPSS 25.0 Statistical Software. Data are expressed as mean ± sem of samples measured in triplicate or more. One-way univariate ANOVA with contrasts was used to test for significant differences between culture conditions. When normality and/or homoscedasticity of the dependent variable were not verified, a Kruskal-Wallis test or the combination of Welch and Brown-Forsythe tests were used for the same purpose. Consequently, multiple comparisons were performed with an appropriate post hoc test (Bonferroni following Kruskal Wallis, Games-Howell following Welch and Brown-Forsythe).

3. Results

3.1. Mammary cell lines of different species are sensitive to EGFR inhibition. We first analysed the relative addiction of different mammary epithelial cell lines to EGFR signaling by adding to the growth medium (G) a highly specific tyrosine kinase inhibitor (AG1478; G+A) at nanomolar concentrations (300 nM). AG1478 was chosen out of three selective EGFR-inhibitors (AG1478, Erlotinib 1μM and Gefitinib 1μM), after comparing their effect in both 2D and in 3D culture, since no differences were seen, either qualitatively (phase contrast 2D and 3D images: Supplementary Fig. S4A and S4B) or quantitatively (nuclei counting and MTT assay: Supplementary Fig. S4C and S4D; p values in Supplementary Tables S2 and S3). As a positive control for inhibition, we used a selective inhibitor of both MEK1 and MEK2, UO126 at 20 μM (G+U). We also used the starving condition (S) to test whether deprivation of all external growth factors influenced cell growth. At 48 h post-treatment cells were recorded (Figure 1A and 1B). Given a high mortality beyond 24 h, BME-UV were recorded only at this timepoint. All cell lines exhibited a clear modification in morphology. BME-UV and MCF-10A, that normally grow as compact colonies in 2D culture, showed a reduction in size and a change in shape; HC11 and NMuMG, that grow as spared cells, showed a decrease in cell number. In collagen, MCF-10A growth did not show organized structures while NMuMG showed extensive 3D branching structures. Both Erk- or EGFR-inhibition abolished growth in 3D. On the other side structures were still visible in the S condition (Figure 1B). BME-UV and HC11 cells did not generate 3D structures in collagen. Cell proliferation, measured by nuclei counting, showed a significant/highly significant reduction in all cell lines cultured with AG1478, UO126 or starved, when compared to control cells in growth medium (Figure 1C and Supplementary Table S2), consistently with a significant decrease of cellular metabolic activity, as confirmed by the MTT assay (Supplementary Fig. S4D; p values in Supplementary Table S3). Similar results were obtained when analyzing the percentage of cells in the G0/G1 phase of the cell cycle. At 16 h post-treatment all lines showed a significant increase *vs* the G control group (Figure 1D; outlined in grey; p values are shown in Supplementary Table S4). A representative example of G0/G1 increase by AG1478 treatment is shown in Fig. 1D, right panel. G0/G1 percentage in the BME-UV line was very variable due to the high level of cell mortality after 16 h of incubation (Figure 1A and 1D and Supplementary Table S4). Inhibiting the PI3K pathway with Wortmannin (100 nM) showed

minor alterations in proliferation (Supplementary Fig. S4C and Supplementary Table S2) and metabolism (Supplementary Fig. S4D and Supplementary Table S3). These data indicate that all mammary epithelial cell lines are highly sensitive to EGFR inhibition. In this setting we could not discriminate whether this response depended on the presence of externally added (in the medium; three out of four cell lines have EGF added to the medium) or internally produced (by the cells) growth factors.

FIGURE 1

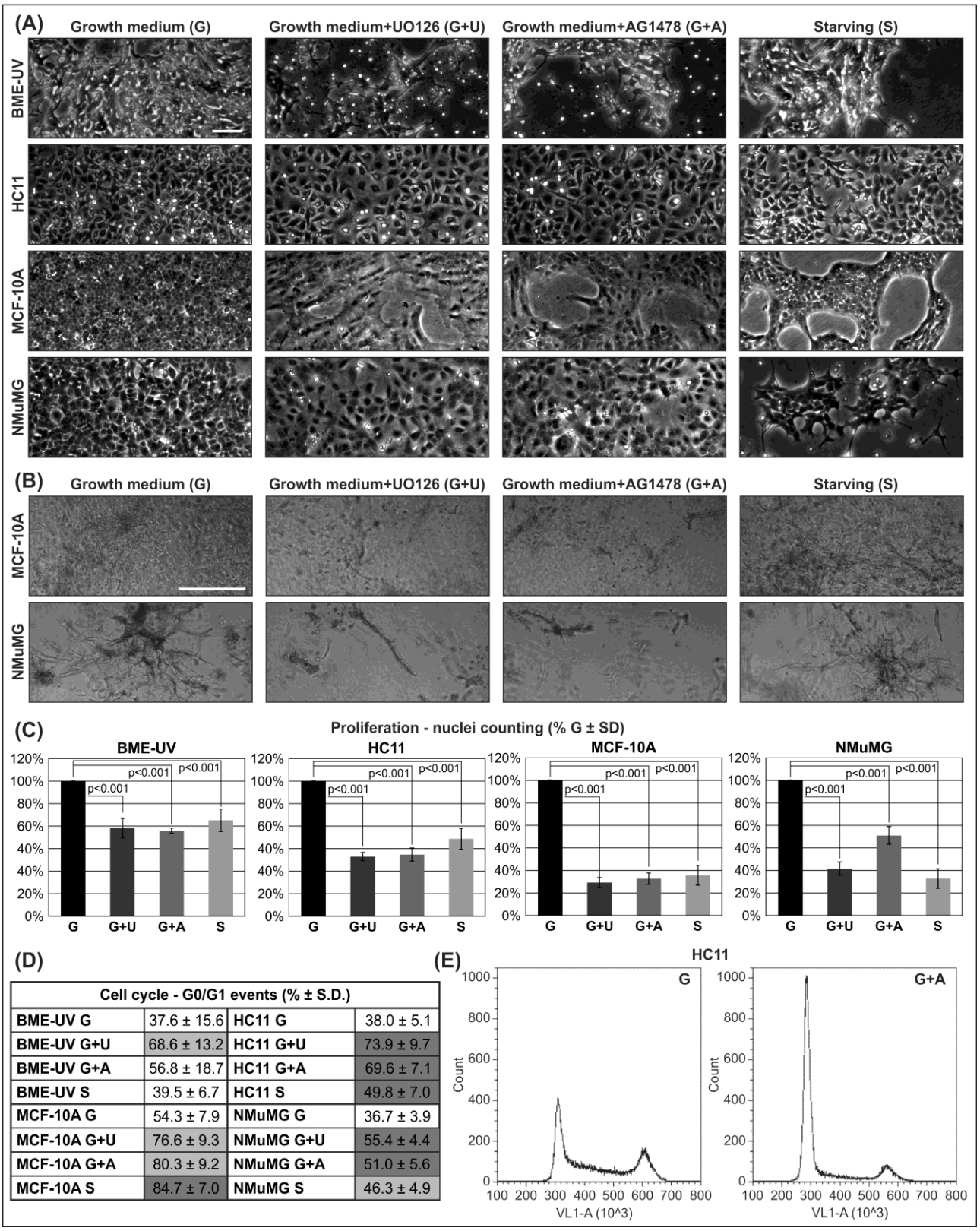

Cell cycle - G0/G1 events (% ± S.D.)			
BME-UV G	37.6 ± 15.6	HC11 G	38.0 ± 5.1
BME-UV G+U	68.6 ± 13.2	HC11 G+U	73.9 ± 9.7
BME-UV G+A	56.8 ± 18.7	HC11 G+A	69.6 ± 7.1
BME-UV S	39.5 ± 6.7	HC11 S	49.8 ± 7.0
MCF-10A G	54.3 ± 7.9	NMuMG G	36.7 ± 3.9
MCF-10A G+U	76.6 ± 9.3	NMuMG G+U	55.4 ± 4.4
MCF-10A G+A	80.3 ± 9.2	NMuMG G+A	51.0 ± 5.6
MCF-10A S	84.7 ± 7.0	NMuMG S	46.3 ± 4.9

Figure 1. EGFR inhibition or starving decrease proliferation and block cell cycle in mammary epithelial cells of different origin. A) Phase contrast images of BME-UV (bovine), HC11 and NMuMG (murine) and MCF-10A (human) mammary epithelial cells cultured for 48 h (24 h for BME-UV) in growth

271 medium (G), growth medium added with AG1748 (G+A), with UO126 (G+U) or in starving medium (S)
272 (see Methods). Bar = 100 µm. **B)** 3D collagen images of NMuMG and MCF-10A mammary epithelial cells
273 treated for 48 h as in Fig. 1A. Bar = 500 µm. **C)** Mammary cells treated as in Fig. 1A were counted (nuclei
274 counting) at 48 h (24 h for BME-UV) post treatment. P values *vs* G are indicated (exact p values in
275 Supplementary Table S2). **D)** Left panel: the percentage of cells in G0/G1 was calculated by FACS analysis
276 after 16 h of treatment. In grey: $p<0.05$ *vs* G. In dark grey: $p<0.001$ *vs* G. Exact p values are indicated in
277 Supplementary Table S4. Right panel: an example of the G0/G1 increase in AG-treated HC11 cells. N/D
278 indicates not done because of high level of mortality after 16 h of treatment.

279

280 **3.2. Mammary cells maintain EGFR-dependent Erk 1/2 activation following external growth**
281 **factor deprivation.** Since UO126 inhibited proliferation and cell cycle in all mammary cell lines to a
282 higher level than serum / growth factors starved cells (S), we decided to verify the Erk 1/2 activation status
283 under the different growth condition and other pathways potentially involved in an EGFR-dependent
284 signaling. We also treated starved cells with AG1478 (S+A), in order to inhibit all external and potential
285 internal EGFR-activating ligands. The selectivity of AG1478 was supported biochemically in MCF-10A
286 cells, by comparison with other inhibitors (Supplementary Fig. S5A and S5B).
287 EGFR was variably phosphorylated in all the lines (Figure 2A, G) and strongly abolished by AG1478
288 (Figure 2A, G+A). In the starving condition, when all external growth factors were removed, EGFR was still
289 phosphorylated (Figure 2A, S). AG1478 almost totally abolished this residual EGFR phosphorylation
290 (Figure 2A, S+A). In MCF-10A the activation of EGFR seemed to be mostly dependent on EGFR-ligands
291 present in the medium. The dephosphorylation of EGFR, under S and S+A conditions, is even more
292 significant, if the levels of total EGFR are considered (Figure 4C). The trend of p Erk 1/2 was substantially
293 consistent with p EGFR.
294 The phosphorylation level of Akt was also negatively affected by EGFR-inhibition (Figure 2, G+A), in all
295 the lines but NMuMG. The phosphorylation of Akt was mainly dependent on external stimuli, since Akt in
296 the starving condition was only slightly dephosphorylated upon AG1478 treatment (Figure 2C, S+A). We
297 finally investigated the phosphorylation of STAT3 and STAT5 upon starving and/or EGFR inhibition.
298 STAT5 did not show phosphorylation under any condition (Figure 2E). STAT3 was phosphorylated in HC11

and MCF-10A lines. The activation of STAT3 did not decrease following EGFR-inhibition (Figure 2D, S and S+A). Since the activation of STAT3 seemed not to depend on EGFR-signaling, and based on the fact that JAK is the activator of STAT signal transductors, we confirmed our evidence in MCF-10A line with a time course of inhibition, by investigating the activation of p STAT3 and p Erk 1/2 in the presence of Ruxolitinib (specific JAK inhibitor). As expected, Ruxolitinib (R) abolished STAT3 but not p Erk 1/2 phosphorylation (Supplementary Fig. S6).

Taken together, these data demonstrate biochemically that an EGFR-dependent signaling is still active in almost all our cell lines, when external stimuli are withdrawn, suggesting that the cells can express EGFR-ligands in starving conditions.

FIGURE 2

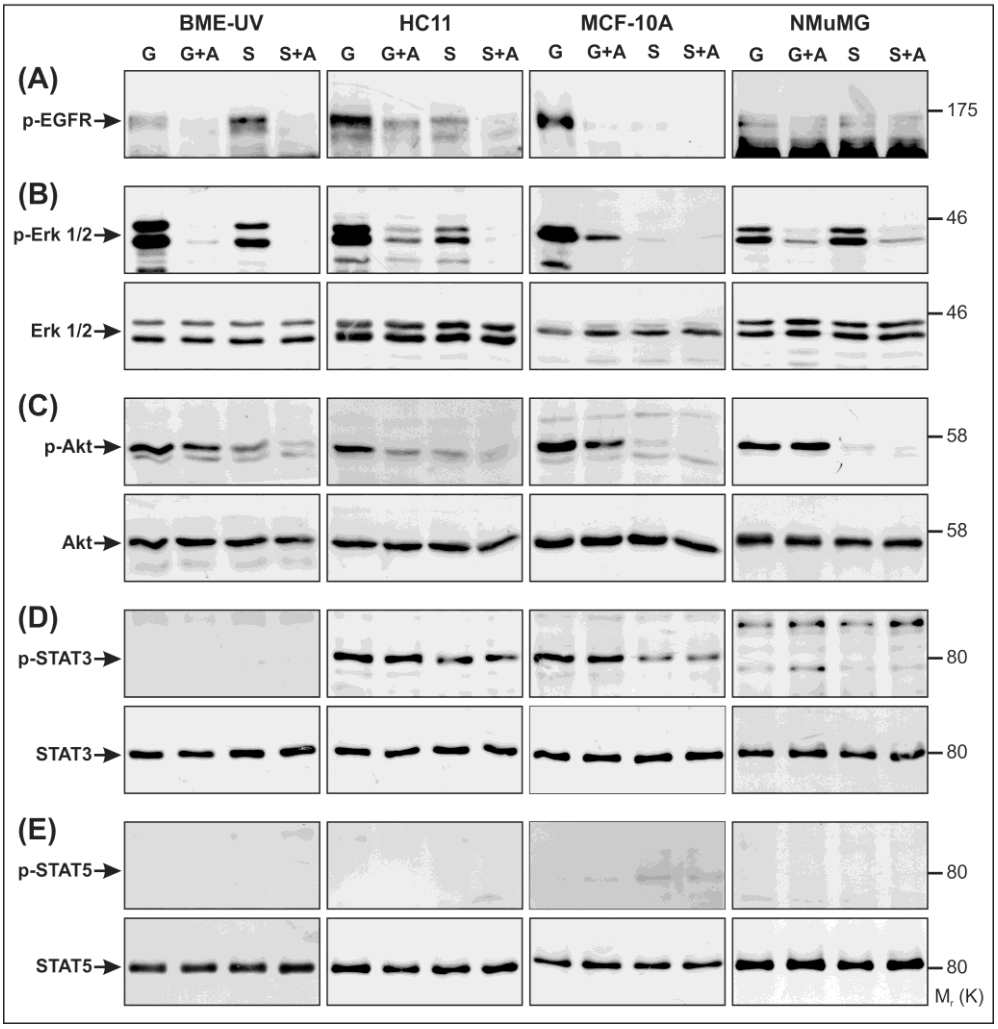

Figure 2. EGFR signaling maintains Erk 1/2 activation in growth factor deprived mammary cells. Western-blot analysis of EGFR (A), Erk 1/2 (B), Akt (C), STAT3 (D) and STAT5 (E) phosphorylation in mammary epithelial cells cultured under the indicated conditions for 16 h or 4 h (for BME-UV, because of

high mortality at 16 h). 30 µg (Erk 1/2, STAT3, STAT5) or 100 µg (EGFR, Akt) of total protein were run on 10% SDS-acrylamide gels. EGFR, Erk 1/2, Akt, STAT3, STAT5 total proteins were used to show comparable protein loading (EGFR total protein in shown in Figure 4C).

3.3. External, but also internal stimuli are responsible for EGFR-induced cell proliferation and survival. We thus analysed whether proliferation, still present in the S condition and possibly determined by internally produced ligands (there are 7 known EGFR ligands), was further reduced upon EGFR inhibition. We also tested whether EGF treatment could recover proliferation/cell cycle in starved cells. No significant differences in the S condition were found, between cells inhibited with AG1748 and cell inhibited with Erlotinib/Gefitinib, either qualitatively (phase contrast 2D and 3D images: Supplementary Fig. S7A and S7B) or quantitatively (nuclei counting and MTT assay: Supplementary Fig. S7C and S7D; p values in Supplementary Tables S5 and S6). Under the S+A condition, when compared to S, BME-UV, HC11 and NMuMG cell lines had a significant reduction in cell number (Figure 3C, Supplementary Table S5), consistent with a decrease of metabolic activity (Supplementary Fig. S7D, Supplementary Table S6), and a significant increase in the G0/G1 population (for the murine lines; Figure 3D and Supplementary Table S7). EGFR- and Erk-inhibition abolished 3D structures in collagen (Figure 3B and Supplementary Fig. S7). EGF treatment recovered proliferation in starved MCF-10A, cell cycle and metabolic activity in MCF-10A and BME-UV (Figures 3C and 3D, Supplementary Fig. S7D, Supplementary Tables S5, S6 and S7). BME-UV, MCF-10A and NMuMG, photographed at 48 h, displayed objects in suspension (Figure 3A), a possible indication of cell death. Abundant debris was also visible among NMuMG and MCF-10A 3D structures in S+A condition (Figure 3B). Analysis of sub-G0 events by FACS showed that EGFR inhibition (G+A *vs* G) significantly increased cell death in BME-UV and NMuMG, while the S+A condition, compared to S, was significantly increased, in three cell lines out of four. A recovery from cell death after treatment with EGF was apparent in BME-UV cells (Figure 3E and Supplementary Table S8). These data indicate that internal EGFR-activating signals are active in mammary cells and sustain proliferation or survival.

FIGURE 3

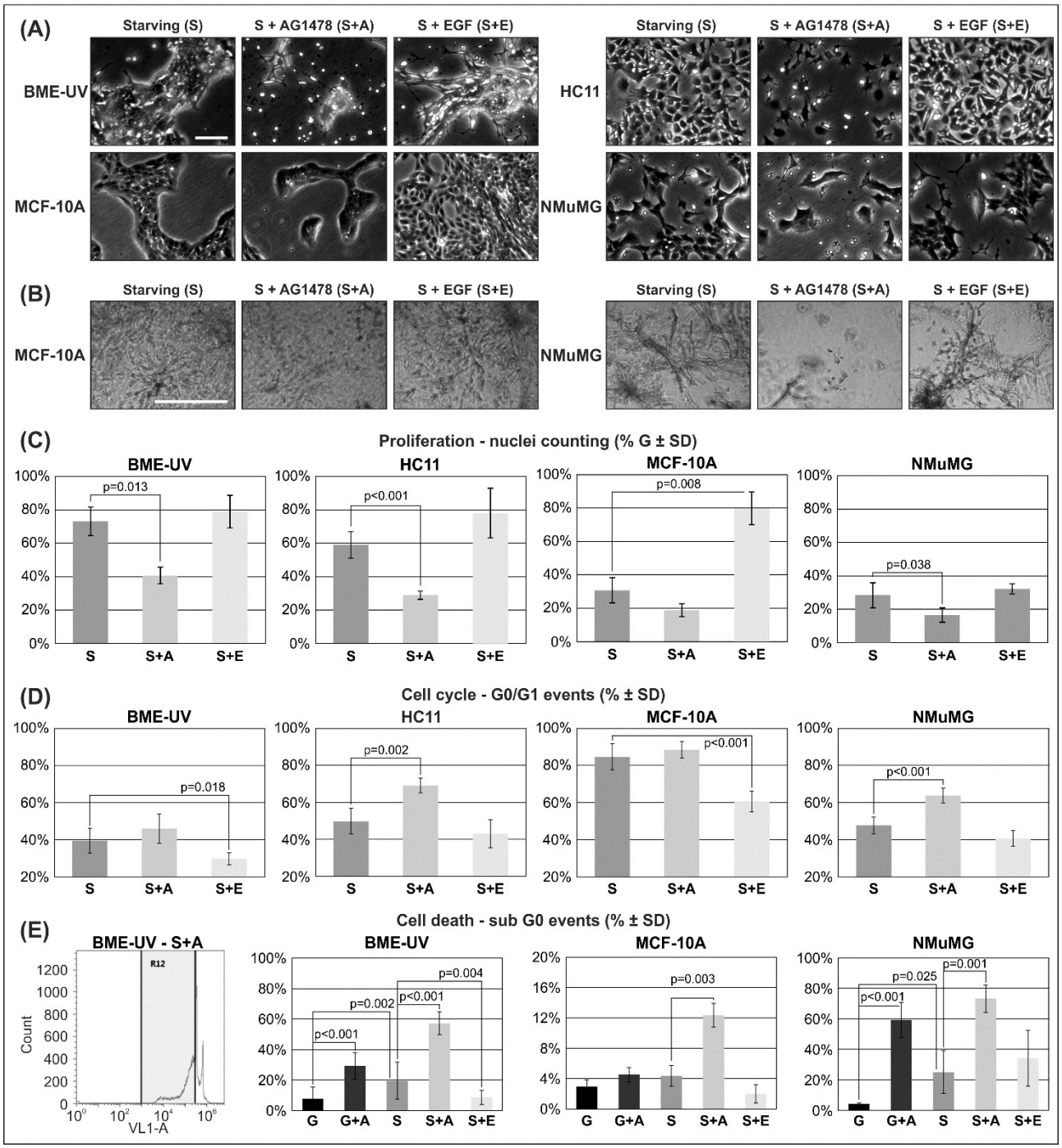

Figure 3. Mammary epithelial cells possess an autocrine EGFR signaling activity sufficient to sustain proliferation, cell cycle and cell viability. A) Phase contrast images of mammary epithelial cells cultured for 48 h in ST and treated with the EGFR inhibitor AG1478 or EGF (10 ng/mL). Bar = 100 µm. **B)** Phase contrast images of NMuMG and MCF-10A mammary epithelial cells cultured in 3D collagen and treated as in Fig. 3A for 48 h. Bar = 500 µm. **C)** Absolute number of cells mammary cells treated as in Fig. 3A. P values *vs* S are indicated (exact p values in Supplementary Table S5). **D)** G0/G1 percentages of cells treated for 16 h as in Fig. 3A. P values *vs* S are indicated (exact p values in Supplementary Table S7). **E)** Left panel:

an example of the sub-G0 population in BME-UV cultured for 16 h in S+A. Right panels: percentages of sub-G0 population determined by FACS analysis after 16 h (BME-UV) or 48 h (MCF-10A and NMuMG). P values *vs* G and *vs* S are indicated (exact p values in Supplementary Table S8).

3.4. Expression and modulation of EGFR ligands, EGFR and Erb-B2 in mammary cells. We thus tested by real-time PCR, the levels of expression of all seven EGFR ligands, EGFR and Erb-B2 (the preferential EGFR hetero-dimerization partner) in cells cultured in growth medium. The mean Cq cycles are indicated in Fig. 4A. Setting an arbitrary cut-off threshold to < 26 Cq, we found that AREG showed a high expression in all cell lines and three of them had two or more "highly" expressed ligands (outlined in gray in Fig. 4A). EGF is not shown because none of the cell lines expressed EGF mRNA (Cq>30). It was then tested whether EGFR ligands, EGFR and Erb-B2, with a Cq<30, were regulated under the different culture conditions. We observed that AREG, EREG and HBEGF were often significantly downregulated by the AG1478 or starving treatments (Figure 4B, Supplementary Figure S8 and Supplementary Table S9). AG1478 treatment in starved cells often significantly reduced the expression of these ligands when compared to the starving treatment alone (Figure 4B and Supplementary Table S9). Given the crucial role of AREG in the development of the ductal tree, we sought to confirm its expression at a protein level. Although AREG was present in all the cell lines (Supplementary Fig. S9), no clear variations were apparent in any of them, upon either starving or EGFR-inhibition (Figure 4C). However, possible variations of AREG shedding were not evaluated in the present study. EGFR and Erb-B2 receptors were not modulated at the mRNA level, to the exception of a slight but significant modulation in MCF-10A (EGFR and Erb-B2; Supplementary Fig. S8 and Supplementary Table S9) and BME-UV cells (Erb-B2 only; Supplementary Figure S8). On the other hand, EGFR and Erb-B2 receptors were upregulated at the protein level, after the G+A, S or S+A treatments (Figure 4C), indicating that the cells respond to both EGFR-inhibition and EGFR-hypoactivation, upregulating EGFR and Erb-B2 post-transcriptionally.

FIGURE 4

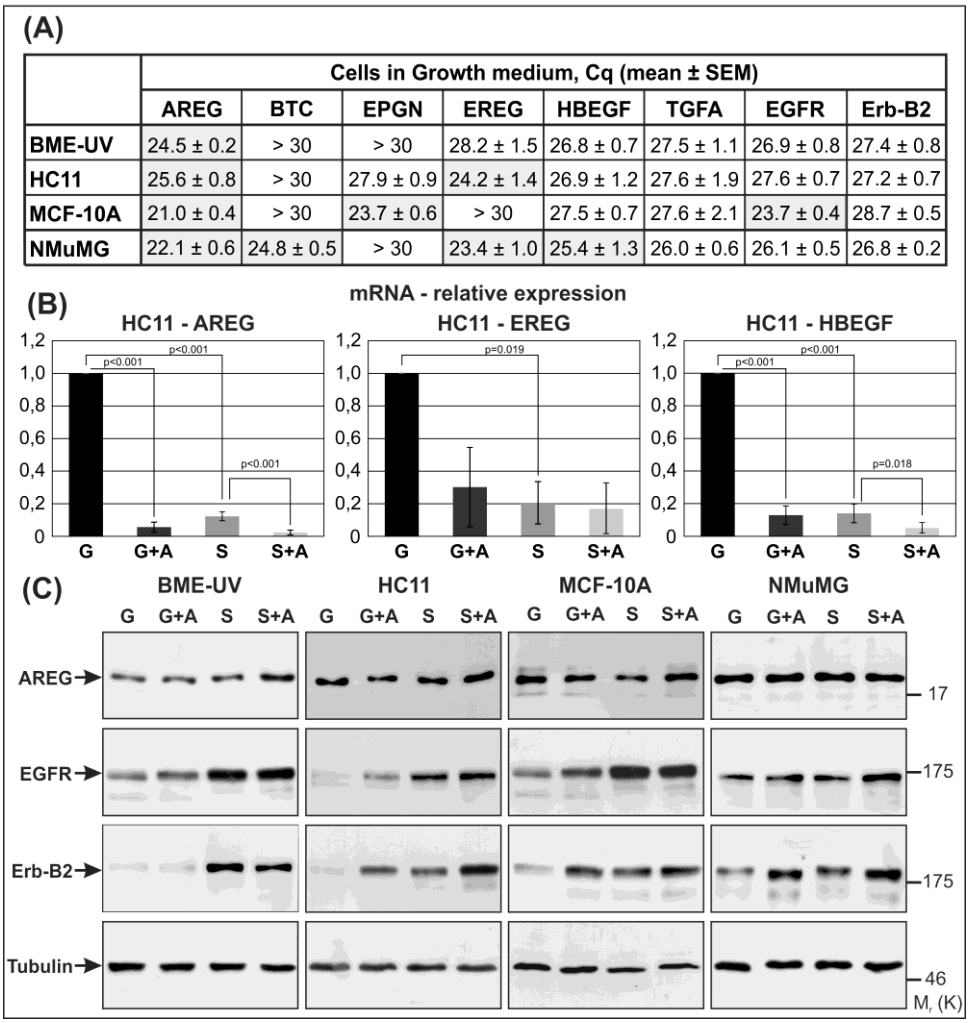

Figure 4. Expression and modulation of EGFR ligands, EGFR and Erb-B2 in mammary epithelial cells. A) Cq mean values ± SEM of six EGFR-ligands, EGFR and Erb-B2 determined by real-time PCR. 7,5 ng of cDNA were used for each amplification reaction. Grey = Cq<26. **B)** Modulation of AREG, EREG and HBEGF in the HC11 cell line cultured for 16 h under the indicated conditions. 7,5 ng of cDNA were processed for each reaction. P values *vs* G and *vs* S are indicated (exact p values in Supplementary Table S9). **C)** Western-blot analysis of AREG, EGFR, and Erb-B2 in mammary epithelial cells cultured under the indicated conditions for 4 h (BME-UV) or 16 h. 30 µg of total protein were run. Tubulin was used to show comparable protein loading.

3.5. EGFR signaling downmodulation reduces the Krt14 negative / Krt18 positive cell population of MCF-10A human mammary cells. EGFR inhibition induced cell death primarily in BME-UV and NMuMG cell lines. Both lines express Krt18, the mouse mammary luminal marker, but not

Krt14, the basal marker. MCF-10A cells, on the other side, express both Krt18 (100% positive expression) and Krt14 (only a cell subpopulation expresses this marker; Supplementary Figure S11 and Qu et al., 2015). We observed that MCF-10A cells treated with G+A or S showed an increase in Krt14 expression both at the mRNA (Figure 5A and Supplementary Table S10) and protein (Figure 5B) levels compared to the untreated G control. When we analyzed Krt14 and Krt18 expression by immunostaining, we found that G+A, G+U, S and S+A treatments increased the area of the well covered by Krt14 cell versus the area covered by all the cells (Krt14/total area; Figures 5C, 5D and Supplementary Table S11). These data indicated that the Krt14 negative population did not grow under these treatments. This effect was reversed upon EGF treatment: in the S+E condition the Krt14/total area ratio returned to G levels (Figure 5D, S+E and Fig. 5C, S+E and Supplementary Table S11). These data indicate that Krt14 negative / Krt18 positive population is highly sensitive to EGFR inhibition.

FIGURE 5

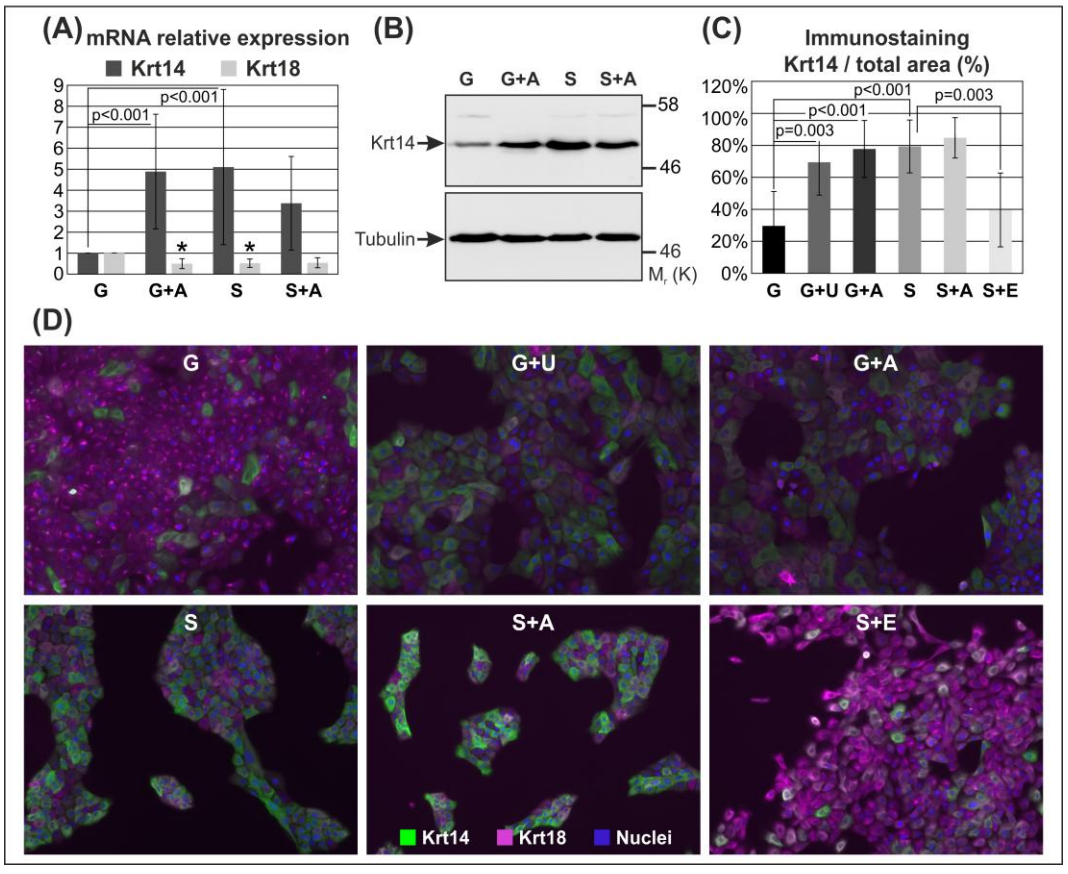

Figure–5. EGFR inhibition in MCF-10A cells reduces the Krt14 negative / Krt18 positive cell population. A) Krt14 and Krt18 mRNA expression in MCF-10A cells cultured under the indicated conditions for 16 h. 7,5 ng of cDNA were used for each amplification reaction. Significant p values *vs* G for

Krt14 are indicated. * denotes significant p values *vs* G for Krt18. Exact p values in Supplementary Table S10. **B)** Krt14 protein expression in MCF-10A cells cultured under the indicated conditions for 16 h. 20 µg of total protein lysates were run. Tubulin shows comparable protein loading in all samples **C)** Krt14 / total area ratio (%) obtained by immunostaining of MCF-10A cells cultured under the indicated conditions for 48 h (see Methods). P values *vs* G and *vs* S are indicated (exact p values in Supplementary Table S11). **D)** Example of composites of immunostaining images stained for Krt14 (green), Krt18 (magenta; adapted for color blindness) and nuclei (blue) in human MCF-10A mammary cells cultured for 48 h under the indicated conditions. Bar = 100 µm. Single images used for the composites and adapted for color blindness, are visible in Supplementary Fig. S10.

4. Discussion

The mammary gland consists of an epithelial cell bilayer surrounded by a mesenchymal stroma, mainly represented by adipocytes in the murine species (Wang & Scherer, 2019). Our current knowledge of this gland reveals that, during the pubertal phase of growth, an endocrine signaling coming from the ovaries induces estrogen receptor positive epithelial cells to release amphiregulin (Ciarloni et al., 2007). This hormone, in turn, activates EGFR in the stromal compartment, enhancing the expression of other growth factors (fibroblast growth factors are the main candidates) that talk back to the epithelial compartment promoting cell proliferation (Sumbal & Koledova, 2019). Both EGFR-/- and AREG-/- mice display arrest of ductal growth and a normal lobuloalveolar development (Ciarloni et al., 2007; Sternlicht et al., 2005). Those and other studies did not however deny the possibility that EGFR expressed also in the epithelial compartment (possibly interacting with Erb-B2) plays an albeit minor role during the ductal development (Andrechek et al., 2005; Jackson-Fisher et al., 2004; Sternlicht et al., 2005), for instance in terms of growth rate or morphology of the mature mammary gland. Nor can be ignored the chance that EGF-like ligands are expressed and act locally, targeting EGFR in the epithelium itself. In summary, an autocrine activity within the epithelial compartment could be hypothesized. In the present work, we adopted different epithelial cells lines, as *in vitro* models for the epithelial compartment, and we sought to demonstrate that these cells can sustain their own proliferation, even in the absence of external stimuli, by activating EGFR (i.e autocrine activity).

Although we observed differences in the responses of the various cell lines, a common behaviour was apparent. The EGFR tyrosine kinase inhibitor tyrphostin (AG1478; IC50 3nM) was used at 300 nM thereby maintaining a unique selectivity over other kinase receptors like Erb-B2 or PDGFR (IC50 100μM) (Fry et al., 1994; Levitzki & Gazit, 1995). This treatment allowed us to properly isolate EGFR-dependent signaling from other non-specific ones. The choice of AG1478 was justified both biologically and biochemically, by comparing its potency with other selective EGFR-receptor, Gefitinib/Iressa (Baselga & Averbuch, 2000) and Erlotinib/Tarceva (Akita & Sliwkowski, 2003). No significant differences were observed between the inhibitory effects of these molecules on proliferation, either qualitatively measured by nuclear counting and MTT assay, or qualitatively evaluated as 2D and 3D growth. AG1478 affected all cell lines by interfering with proliferation, as evidenced by reduced cell count, block of cells in the G0/G1 phase of the cell cycle and impaired 3D-growth. The BME-UV (after 16 h) and NMuMG (after 48 h) cell lines also exhibited an increase in the sub-G0 population, indicative of cell death. At this point we could not discriminate whether EGFR activation was elicited by EGFR-ligands coming from the medium (EGF is present in the culture medium for BME-UV, HC11 and MCF-10A) or by the cells themselves. The cell lines used in the present work are moreover variably responsive to steroid hormones. HC11 cells were found Estrogen Receptor positive (ER+) both at mRNA and protein level (Hedengran Faulds et al., 2004; Sornapudi et al., 2018; Williams et al., 2009), BME-UV cells are responsive to both estrogen and progesterone, although their molecular signature has not been elucidated (Sobolewska et al., 2011), nor NMuMG line was described with that respect. MCF-10A were reported to be ER- and Progesterone Receptor positive (PR+) only in microarray analysis (Charafe-Jauffret et al., 2006; Hevir et al., 2011; Moran et al., 2000). We partially confirmed these previous findings by gene expression analysis, except for a low but detectable level of ERα mRNA in MCF-10A cells, as well as in the NMuMG line (data not shown). Therefore, the chance that external factors present in the growth media induce the cells to proliferate, potentially activating ER or other receptors, cannot be excluded. This is relevant especially because ERα affects the synthesis of AREG (and potentially other EGF-like factors) in the mammary epithelium. All that considered, we deprived the cells of all ligands and hormones present in the medium and added AG1478. Comparing these treatments, we observed a further reduction in cell number in HC11, NMuMG and BME-UV, and an increase in the G0/G1 events in HC11 and NMuMG. We also detected an increase in the sub-G0 population in BME-UV, MCF-

453 10A and NMuMG. Adding EGF alone to the starving condition either increased cell number (in MCF-10A
454 and to a lesser extent HC11), reduced G0/G1 events (in BME-UV and MCF-10A) or reduced cell death (in
455 BME-UV and MCF-10A). Therefore, all cell lines show that EGFR signaling activated by factors either
456 present in the medium or produced by the cells themselves, plays a role in proliferation or survival.
457 Different pathways are known to be variably activated downstream of Erb-B receptors, but a good evidence
458 supported our main interest in Erk 1/2. EGFR is a strong activator of Ras/Erk pathway, by means of multiple
459 binding sites for Grb2 and SHC. Moreover, the ductal branching triggered *in vitro* by EGF-like factors
460 depends on p Erk, in the murine species (Camacho Leal et al., 2012; Fata et al., 2007; Kariagina et al., 2010).
461 The analysis of the status of Erk 1/2 phosphorylation in our cells deprived of any external growth factor, the
462 starving condition, showed that phosphor-Erk was still elevated (to the exception of MCF-10A) and that
463 AG1478 abolished this signaling almost completely. This trend was substantially aligned with the
464 phosphorylation (i.e activation) of EGFR and indicates that cells retain active EGFR signaling when all
465 external growth factors have been withdrawn, by producing their own EGFR-ligands. The activation of p Erk
466 in AG1478-treated cells is further abolished when external factors are withdrawn (compare the G+A with
467 S+A lanes in HC11 and MCF-10A cells, Fig. 2B). We can therefore conclude that the Erk activity is, to some
468 extent, independent of EGFR signaling which is consistent with the multiple signaling pathways relying on
469 this kinase. EGFR is also a potential activator of PI3K/Akt pathway, and our data confirms that link,
470 showing that Akt phosphorylation is partially abolished in the presence of AG1478, in all the lines except
471 NMuMG. On the other hand, differences between S and S+A were barely visible. It is possible that this
472 pathway is activated in the context of a hypothetical autocrine, EGFR-mediated signaling in our cell lines,
473 but p Akt plays a minor role compared to p Erk, consistently with the mild effects upon wortmannin
474 treatment. It is also possible that these two pathways play complementary roles in mammary morphogenesis,
475 as previously demonstrated for MCF-10A cells (Tang et al., 2014; Tarcic et al., 2012). According to our
476 results, there are no links between p EGFR and the activation of p STAT3 (apparent in HC11 and MCF-10A)
477 or p STAT5 (evidenced in none of the lines) in the lines here investigated.
478 When we determined the expression of all seven EGFR-ligands we found that AREG mRNA was present at
479 high levels in all the cell lines, with other factors (to the exception of EGF) often reaching considerable
480 levels of expression. We also observed a strong downregulation of some ligands (AREG, EREG, HBEGF

481 and BTC) when medium derived factors were removed or EGFR signaling was inhibited. These data
482 indicated that the gene expression of several EGFR ligands is regulated in a fashion consistent with cell
483 proliferation and survival, suggesting that these factors could be the mediators of the autocrine activity we
484 demonstrated, in a similar way to what was described in breast cancer by (Zhou et al., 2014). The ligands for
485 the EGFR receptor have been described as immediate early genes with fast regulation kinetics that depend on
486 the protein kinase C and/or extracellular-signal-regulated kinase (Barnard et al., 1994; Berasain & Avila,
487 2014; Kerpedjieva et al., 2012; Shirakata et al., 2010; Taylor et al., 2014). It is therefore likely that, in our
488 cellular system, EGFR signaling maintain these ligands upregulated, by promoting Erk 1/2 phosphorylation.
489 A detailed study of the signaling regulating these ligands in the mammary compartment is underway.
490 Surprisingly, AREG protein levels seemed to be unaffected either by starving condition or EGFR-inhibition.
491 Although we cannot rationally explain this evidence, it could be speculated that only the release of active
492 AREG (not measured in the present study) is impaired by EGFR-inhibition. Another possibility is that only
493 AREG gene expression is regulated, and other EGF-like effectors are involved downstream of EGFR, or that
494 the half-life of AREG is longer than 48 h in the lines here examined (current experiments are underway). On
495 the other side, EGFR and Erb-B2 showed that their protein, but not their mRNA was upregulated under the
496 G+A, S or S+A treatments. This finding was not surprising, since it was proved and extensively reviewed
497 that tyrosine kinase receptors become downregulated when activated by their own ligands (Darcy et al.,
498 1999; Edery et al., 1989; Waterman & Yarden, 2001).
499 According the results published herein, proliferation and activation of Erk 1/2, in MCF-10A cells, almost
500 exclusively relied on EGF included in the growth medium. These data were in marked contrast with other
501 lines, that self-sustained in starving condition, by activating EGFR-Erk 1/2 signaling pathway. We therefore
502 investigated which characteristics could make MCF-10A unique over the other lines. HC11 are all Krt14
503 positive, BME-UV and NMuMG are all Krt18 positive, while MCF-10A express markers of both the basal
504 and luminal compartments (Qu et al., 2015). MCF-10A cells treated with AG1478, UO126 or starved
505 exhibited a strong reduction of the Krt14 negative / Krt18 positive cell population, which was restored upon
506 EGF treatment almost back to the growth condition. Our data are in line with previous observations that a
507 basal cell fate might be supported in the absence of EGF (Deugnier et al., 1999). In MCF10A cells AREG
508 promotes an epithelial cell fate, by activating EGFR-ERK signaling even if less strongly than EGF. In the

same study, Krt14 gene was differentially expressed in AREG- or EGF-stimulated cells (Fukuda et al., 2016). Those previous results might also explain why MCF-10A cells, that express high levels of AREG mRNA and protein, did not maintain proliferation or Erk 1/2 phosphorylation in our experiments, when EGF was removed from the medium. All in all, the results about cell proliferation, cell death and Krt14/18 expression, together with previous findings, suggest that EGFR signaling is important for the viability of Krt18 cells (NMuMG and BME-UV) negative for Krt14 (MCF-10A). The decrease of such a population might explain why an EGFR-dependent autocrine signaling was not apparent in the MCF-10A here examined.

Although our data were obtained from four cell lines of different source, we are aware that our demonstration of a potential autocrine signaling is "indirect", being focused on the potential of cells to survive without external growth factors. This first, significant evidence encourages a more direct demonstration. We also acknowledge that the observed effect may depend on the immortalization process that has selected "EGFR dependent" cells and that immortalized lines are not a realistic model of the real mammary epithelium. We are currently addressing these issues by using primary, animal-isolated mammary cells from different sources. In this regard, the first data obtained in the swine and bovine are promising and may prove that our assessment is also correct in an *ex vivo* system.

In conclusion, we identified a gap in the scientific background, whereby stromal EGFR certainly plays a major role in the pubertal development of the mammary gland, but the contribution of its epithelial counterpart is not elucidated. We have shown that EGFR is expressed by several epithelial cell lines, here used as *in vitro* model of the mammary epithelium, and that p EGFR (activated receptor) triggers a signaling that promotes the proliferation and survival of cells, even in the absence of external stimuli (i.e factors included in the medium), mainly by activating Erk 1/2. This proves the existence of an autocrine signal among mammary epithelial cells *in vitro* and lays the foundations for further studies *ex vivo*.

Conflict of interest: The authors declare no conflict of interest.

Akita, R. W., & Sliwkowski, M. X. (2003). Preclinical studies with erlotinib (Tarceva). *Seminars in Oncology*, *30*(3 SUPPL. 7), 15–24. https://doi.org/10.1016/S0093-7754(03)70011-6

537 Andrechek, E. R., White, D., & Muller, W. J. (2005). Targeted disruption of ErbB2/Neu in the mammary
538 epithelium results in impaired ductal outgrowth. *Oncogene*, *24*(5), 932–937.
539 https://doi.org/10.1038/sj.onc.1208230
540 Barnard, J. A., Graves-Deal, R., Pittelkowll, M. R., Duboisn, R., Cooklll, P., Ramseys, G. W., Bishop, P. R.,
541 Damstrupn, L., & Coffefl, R. J. (1994). Auto-and Cross-induction within the Mammalian Epidermal
542 Growth Factor-related Peptide Family. *Journal of Biological Chemistry*, *269*(36), 22817–22822.
543 Baselga, J., & Averbuch, S. D. (2000). ZD1839 ('Iressa') 1,2 as an Anticancer Agent. *Drugs*, *60*(SUPPL. 1),
544 33–40.
545 Berasain, C., & Avila, M. A. (2014). Amphiregulin. *Seminars in Cell and Developmental Biology*, *28*, 31–
546 41. https://doi.org/10.1016/j.semcdb.2014.01.005
547 Camacho Leal, M. del P., Pincini, A., Tornillo, G., Fiorito, E., Bisaro, B., Di Luca, E., Turco, E., Defilippi,
548 P., & Cabodi, S. (2012). p130Cas Over-Expression Impairs Mammary Branching Morphogenesis in
549 Response to Estrogen and EGF. *PLoS ONE*, *7*(12), e49817.
550 https://doi.org/10.1371/journal.pone.0049817
551 Charafe-Jauffret, E., Ginestier, C., Monville, F., Finetti, P., Adélaïde, J., Cervera, N., Fekairi, S., Xerri, L.,
552 Jacquemier, J., Birnbaum, D., & Bertucci, F. (2006). Gene expression profiling of breast cell lines
553 identifies potential new basal markers. *Oncogene*, *25*(15), 2273–2284.
554 https://doi.org/10.1038/sj.onc.1209254
555 Ciarloni, L., Mallepell, S., & Brisken, C. (2007). Amphiregulin is an essential mediator of estrogen receptor
556 alpha function in mammary gland development. *Proceedings of the National Academy of Sciences of*
557 *the United States of America*, *104*(13), 5455–5460. https://doi.org/10.1073/pnas.0611647104
558 Coleman, S., Silberstein, G. B., & Daniel, C. W. (1988). Ductal morphogenesis in the mouse mammary
559 gland: Evidence supporting a role for epidermal growth factor. *Developmental Biology*, *127*(2), 304–
560 315. https://doi.org/10.1016/0012-1606(88)90317-X
561 D'Cruz, C. M., Moody, S. E., Master, S. R., Hartman, J. L., Keiper, E. A., Imielinski, M. B., Cox, J. D.,
562 Wang, J. Y., Ha, S. I., Keister, B. A., & Chodosh, L. A. (2002). Persistent Parity-Induced Changes in
563 Growth Factors, TGF-β3, and Differentiation in the Rodent Mammary Gland. *Molecular*
564 *Endocrinology*, *16*(9), 2034–2051. https://doi.org/10.1210/me.2002-0073

565 Darcy, K. M., Wohlhueter, A. L., Zangani, D., Vaughan, M. M., Russell, J. A., Masso-Welch, P. A., Varela,
566 L. M., Shoemaker, S. F., Horn, E., Lee, P.-P. H., Huang, R.-Y., & Ip, M. M. (1999). Selective changes
567 in EGF receptor expression and function during the proliferation, differentiation and apoptosis of
568 mammary epithelial cells. *European Journal of Cell Biology*, *78*(7), 511–523.
569 https://doi.org/10.1016/S0171-9335(99)80077-6
570 Darcy, K. M., Zangani, D., Wohlhueter, A. L., Huang, R.-Y., Vaughan, M. M., Russell, J. A., & Ip, M. M.
571 (2000). Changes in ErbB2 (her-2/neu), ErbB3, and ErbB4 during Growth, Differentiation, and
572 Apoptosis of Normal Rat Mammary Epithelial Cells. *Journal of Histochemistry & Cytochemistry*,
573 *48*(1), 63–80. https://doi.org/10.1177/002215540004800107
574 Deugnier, M. A., Faraldo, M. M., Rousselle, P., Thiery, J. P., & Glukhova, M. A. (1999). Cell-extracellular
575 matrix interactions and EGF are important regulators of the basal mammary epithelial cell phenotype.
576 *Journal of Cell Science*, *112*(7), 1035 LP – 1044. http://jcs.biologists.org/content/112/7/1035.abstract
577 DiAugustine, R. P., Richards, R. G., & Sebastian, J. (1997). EGF-Related Peptides and Their Receptors in
578 Mammary Gland Development. *Journal of Mammary Gland Biology and Neoplasia*, *2*(2), 109–117.
579 https://doi.org/10.1023/A:1026395513038
580 Edery, M., Pang, K., Larson, L., & Nandi, S. (1989). Turnover of epidermal growth factor binding sites in
581 mouse mammary epithelial cells. *Biomedicine & Pharmacotherapy*, *43*(5), 361–368.
582 https://doi.org/10.1016/0753-3322(89)90062-0
583 Fata, J. E., Mori, H., Ewald, A. J., Zhang, H., Yao, E., Werb, Z., & Bissell, M. J. (2007). The MAPK ERK-
584 1,2 pathway integrates distinct and antagonistic signals from TGFα and FGF7 in morphogenesis of
585 mouse mammary epithelium. *Developmental Biology*, *306*(1), 193–207.
586 https://doi.org/10.1016/j.ydbio.2007.03.013
587 Fry, D. W., Kraker, A. J., Mcmichael, A., Ambroso, L. A., Nelson, J. M., Leopold, W. R., Conners, R. W., &
588 Bridges, A. J. (1994). A Specific Inhibitor of the Epidermal Growth Factor Receptor Tyrosine Kinase.
589 *Science*, *265*(5175), 1093–1095. https://doi.org/10.1126/science.8066447
590 Fukuda, S., Nishida-Fukuda, H., Nanba, D., Nakashiro, K. I., Nakayama, H., Kubota, H., & Higashiyama, S.
591 (2016). Reversible interconversion and maintenance of mammary epithelial cell characteristics by the
592 ligand-regulated EGFR system. *Scientific Reports*, *6*(1), 1–16. https://doi.org/10.1038/srep20209

593 Harris, R. C., Chung, E., & Coffey, R. J. (2003). EGF receptor ligands. *Experimental Cell Research*, *284*(1),
594 2–13. https://doi.org/10.1016/S0014-4827(02)00105-2
595 Hedengran Faulds, M., Olsen, H., Helguero, L. A., Gustafsson, J.-åke, & Haldosé, L. N. (2004). Estrogen
596 Receptor Functional Activity Changes during Differentiation of Mammary Epithelial Cells. *Molecular*
597 *Endocrinology*, *18*(2), 412–421. https://doi.org/10.1210/me.2003-0290
598 Hevir, N., Trošt, N., Debeljak, N., & Rižner, T. L. (2011). Expression of estrogen and progesterone receptors
599 and estrogen metabolizing enzymes in different breast cancer cell lines. *Chemico-Biological*
600 *Interactions*, *191*, 206–216. https://doi.org/10.1016/j.cbi.2010.12.013
601 Jackson-Fisher, A. J., Bellinger, G., Ramabhadran, R., Morris, J. K., Lee, K.-F., & Stern, D. F. (2004).
602 ErbB2 is required for ductal morphogenesis of the mammary gland. *Proceedings of the National*
603 *Academy of Sciences*, *101*(49), 17138–17143. https://doi.org/10.1073/pnas.0407057101
604 Jenkins, E. C., Debnath, S., Gundry, S., Gundry, S., Uyar, U., & Fata, J. E. (2012). Intracellular pH
605 regulation by Na+/H+ exchanger-1 (NHE1) is required for growth factor-induced mammary branching
606 morphogenesis. *Developmental Biology*, *365*(1), 71–81. https://doi.org/10.1016/j.ydbio.2012.02.010
607 Kariagina, A., Xie, J., Leipprandt, J. R., & Haslam, S. Z. (2010). Amphiregulin Mediates Estrogen,
608 Progesterone, and EGFR Signaling in the Normal Rat Mammary Gland and in Hormone-Dependent
609 Rat Mammary Cancers. *Hormones and Cancer*, *1*(5), 229–244. https://doi.org/10.1007/s12672-010-
610 0048-0
611 Kerpedjieva, S. S., Kim, D. S., Barbeau, D. J., & Tamama, K. (2012). EGFR ligands drive multipotential
612 stromal cells to produce multiple growth factors and cytokines via early growth response-1. *Stem Cells*
613 *and Development*, *21*(13), 2541–2551. https://doi.org/10.1089/scd.2011.0711
614 Levitzki, A., & Gazit, A. (1995). Tyrosine kinase inhibition: an approach to drug development. *Science*,
615 *267*(5205), 1782–1788. https://doi.org/10.1126/science.7892601
616 Luetteke, N. C., Qiu, T. H., Fenton, S. E., Troyer, K. L., Riedel, R. F., Chang, A., & Lee, D. C. (1999).
617 Targeted inactivation of the EGF and amphiregulin genes reveals distinct roles for EGF receptor
618 ligands in mouse mammary gland development. *Development (Cambridge, England)*, *126*(12), 2739–
619 2750. http://www.ncbi.nlm.nih.gov/pubmed/10331984
620 Macias, H., & Hinck, L. (2012). Mammary gland development. *Wiley Interdisciplinary Reviews.*

621 *Developmental Biology*, *1*(4), 533–557. https://doi.org/10.1002/wdev.35
622 Moran, T. J., Gray, S., Mikosz, C. A., & Conzen, S. D. (2000). The Glucocorticoid Receptor Mediates a
623 Survival Signal in Human Mammary Epithelial Cells 1. *Cancer Research*, *60*(4), 867–872.
624 Qu, Y., Han, B., Yu, Y., Yao, W., Bose, S., Karlan, B. Y., Giuliano, A. E., & Cui, X. (2015). Evaluation of
625 MCF10A as a Reliable Model for Normal Human Mammary Epithelial Cells. *PLOS ONE*, *10*(7),
626 e0131285. https://doi.org/10.1371/journal.pone.0131285
627 Schroeder, J. A., & Lee, D. C. (1998). Dynamic expression and activation of ERBB receptors in the
628 developing mouse mammary gland. *Cell Growth & Differentiation : The Molecular Biology Journal of*
629 *the American Association for Cancer Research*, *9*(6), 451–464.
630 http://www.ncbi.nlm.nih.gov/pubmed/9663464
631 Shirakata, Y., Tokumaru, S., Sayama, K., & Hashimoto, K. (2010). Auto- and cross-induction by betacellulin
632 in epidermal keratinocytes. In *Journal of Dermatological Science* (Vol. 58, Issue 2, pp. 162–164).
633 Elsevier. https://doi.org/10.1016/j.jdermsci.2010.03.016
634 Simian, M., Hirai, Y., Navre, M., Werb, Z., Lochter, A., & Bissell, M. J. (2001). The interplay of matrix
635 metalloproteinases, morphogens and growth factors is necessary for branching of mammary epithelial
636 cells. *Development*, *128*(16), 3117–3131. http://www.ncbi.nlm.nih.gov/pubmed/11688561
637 Sisto, M., Lorusso, L., Ingravallo, G., & Lisi, S. (2017). Exocrine Gland Morphogenesis: Insights into the
638 Role of Amphiregulin from Development to Disease. *Archivum Immunologiae et Therapiae*
639 *Experimentalis*, *65*(6), 477–499. https://doi.org/10.1007/s00005-017-0478-2
640 Sobolewska, A., Motyl, T., & Gajewska, M. (2011). Role and regulation of autophagy in the development of
641 acinar structures formed by bovine BME-UV1 mammary epithelial cells. *European Journal of Cell*
642 *Biology*, *90*, 854–864. https://doi.org/10.1016/j.ejcb.2011.06.007
643 Sornapudi, T. R., Nayak, R., Guthikonda, P. K., Pasupulati, A. K., Kethavath, S., Uppada, V., Mondal, S.,
644 Yellaboina, S., & Kurukuti, S. (2018). Comprehensive profiling of transcriptional networks specific for
645 lactogenic differentiation of HC11 mammary epithelial stem-like cells. *Scientific Reports*, *8*(11777).
646 https://doi.org/10.1038/s41598-018-30122-4
647 Spivak-Kroizman, T., Rotin, D., Pinchasi, D., Ullrich, A., Schlessinger, J., & Lax, I. (1992).
648 Heterodimerization of c-erbB2 with different epidermal growth factor receptor mutants elicits

649 stimulatory or inhibitory responses. *The Journal of Biological Chemistry*, *267*(12), 8056–8063.
650 http://www.ncbi.nlm.nih.gov/pubmed/1349015
651 Sternlicht, M. D., Sunnarborg, S. W., Kouros-Mehr, H., Yu, Y., Lee, D. C., & Werb, Z. (2005). Mammary
652 ductal morphogenesis requires paracrine activation of stromal EGFR via ADAM17-dependent shedding
653 of epithelial amphiregulin. *Development*, *132*(17), 3923–3933. https://doi.org/10.1242/dev.01966
654 Sumbal, J., & Koledova, Z. (2019). FGF signaling in mammary gland fibroblasts regulates multiple
655 fibroblast functions and mammary epithelial morphogenesis. *Development*, *146*(23), dev185306.
656 https://doi.org/10.1242/dev.185306
657 Tang, W. Y. Y., Beckett, A. J., Prior, I. A., Coulson, J. M., Urbé, S., & Clague, M. J. (2014). Plasticity of
658 mammary cell boundaries governed by EGF and actin remodeling. *Cell Reports*, *8*(6), 1722–1730.
659 https://doi.org/10.1016/j.celrep.2014.08.026
660 Tarcic, G., Avraham, R., Pines, G., Amit, I., Shay, T., Lu, Y., Zwang, Y., Katz, M., Ben- Chetrit, N.,
661 Jacob- Hirsch, J., Virgilio, L., Rechavi, G., Mavrothalassitis, G., Mills, G. B., Domany, E., & Yarden,
662 Y. (2012). EGR1 and the ERK- ERF axis drive mammary cell migration in response to EGF. *The*
663 *FASEB Journal*, *26*(4), 1582–1592. https://doi.org/10.1096/fj.11-194654
664 Taylor, S. R., Markesbery, M. G., & Harding, P. A. (2014). Heparin-binding epidermal growth factor-like
665 growth factor (HB-EGF) and proteolytic processing by a disintegrin and metalloproteinases (ADAM):
666 A regulator of several pathways. *Seminars in Cell and Developmental Biology*, *28*, 22–30.
667 https://doi.org/10.1016/j.semcdb.2014.03.004
668 Thiel, G., & Cibelli, G. (2002). Regulation of life and death by the zinc finger transcription factor Egr-1.
669 *Journal of Cellular Physiology*, *193*(3), 287–292. https://doi.org/10.1002/jcp.10178
670 Wang, Q. A., & Scherer, P. E. (2019). Remodeling of Murine Mammary Adipose Tissue during Pregnancy,
671 Lactation, and Involution. *Journal of Mammary Gland Biology and Neoplasia*, *24*(3), 207–212.
672 https://doi.org/10.1007/s10911-019-09434-2
673 Waterman, H., & Yarden, Y. (2001). Molecular mechanisms underlying endocytosis and sorting of ErbB
674 receptor tyrosine kinases. *FEBS Letters*, *490*(3), 142–152. https://doi.org/10.1016/S0014-
675 5793(01)02117-2
676 Wiesen, J. F., Young, P., Werb, Z., Cunha, G. R., Mandel, R., Krajewski, S., Reed, J. C., & Rosen, J. M.

(1999). Signaling through the stromal epidermal growth factor receptor is necessary for mammary ductal development. *Development*, *126*(2), 335–344. http://www.ncbi.nlm.nih.gov/pubmed/9847247

Williams, C., Helguero, L., Edvardsson, K., Haldosén, L. A., & Gustafsson, J. Å. (2009). Gene expression in murine mammary epithelial stem cell-like cells shows similarities to human breast cancer gene expression. *Breast Cancer Research*, *11*(3), R26. https://doi.org/10.1186/bcr2256

Zhang, X., Martinez, D., Koledova, Z., Qiao, G., Streuli, C. H., & Lu, P. (2014). FGF ligands of the postnatal mammary stroma regulate distinct aspects of epithelial morphogenesis. *Development*, *141*(17), 3352–3362. https://doi.org/10.1242/dev.106732

Zhou, Z. N., Sharma, V. P., Beaty, B. T., Roh-Johnson, M., Peterson, E. A., Van Rooijen, N., Kenny, P. A., Wiley, H. S., Condeelis, J. S., & Segall, J. E. (2014). Autocrine HBEGF expression promotes breast cancer intravasation, metastasis and macrophage-independent invasion in vivo. *Oncogene*, *33*(29), 3784–3793. https://doi.org/10.1038/onc.2013.363